Acta Pharmaceutica Sinica B 2024;14(1):190−206

Chinese Pharmaceutical Association
Institute of Materia Medica, Chinese Academy of Medical Sciences

Acta Pharmaceutica Sinica B

www.elsevier.com/locate/apsb
www.sciencedirect.com

ORIGINAL ARTICLE

High-throughput screening of novel TFEB agonists in protecting against acetaminophen-induced liver injury in mice

Xiaojuan Chao[a,*,†], Mengwei Niu[a], Shaogui Wang[a], Xiaowen Ma[a], Xiao Yang[a,b], Hua Sun[a,c], Xujia Hu[a], Hua Wang[a,c], Li Zhang[d], Ruili Huang[d], Menghang Xia[d], Andrea Ballabio[e,f,g], Hartmut Jaeschke[a], Hong-Min Ni[a], Wen-Xing Ding[a,h,*]

[a]*Department of Pharmacology, Toxicology and Therapeutics, University of Kansas Medical Center, Kansas City, KS 66160, USA*
[b]*NMPA Key Laboratory for Research and Evaluation of Drug Metabolism & Guangdong Provincial Key Laboratory of New Drug Screening, School of Pharmaceutical Sciences, Southern Medical University, Guangzhou 510515, China*
[c]*Department of Oncology, the First Affiliated Hospital of Anhui Medical University, Anhui Medical University, Hefei 230032, China*
[d]*National Center for Advancing Translational Sciences, National Institutes of Health, Bethesda, MD 20892, USA*
[e]*Telethon Institute of Genetics and Medicine, TIGEM, Pozzuoli, Naples 80131, Italy*
[f]*Medical Genetics, Department of Translational Medicine, Federico II University, Naples 80131, Italy*
[g]*Department of Molecular and Human Genetics, Baylor College of Medicine, Houston, TX 77030, USA*
[h]*Department of Internal Medicine, Division of Gastroenterology, Hepatology & Motility, University of Kansas Medical Center, Kansas City, KS 66160, USA*

Received 25 August 2023; received in revised form 12 September 2023; accepted 15 September 2023

KEY WORDS

Autophagy;
DILI;
Drug screening;
Hepatotoxicity;

Abstract Macroautophagy (referred to as autophagy hereafter) is a major intracellular lysosomal degradation pathway that is responsible for the degradation of misfolded/damaged proteins and organelles. Previous studies showed that autophagy protects against acetaminophen (APAP)-induced injury (AILI) *via* selective removal of damaged mitochondria and APAP protein adducts. The lysosome is a critical organelle sitting at the end stage of autophagy for autophagic degradation *via* fusion with autophagosomes. In the

*Corresponding authors.
E-mail addresses: wxding@kumc.edu (Wen-Xing Ding), chaoxj3@mail.sysu.edu.cn (Xiaojuan Chao).
[†]Current affiliation: Institute of Precision Medicine, the First Affiliated Hospital, Sun Yat-sen University, Guangzhou 510515, China.
Peer review under the responsibility of Chinese Pharmaceutical Association and Institute of Materia Medica, Chinese Academy of Medical Sciences.

https://doi.org/10.1016/j.apsb.2023.10.017
2211-3835 © 2024 The Authors. Published by Elsevier B.V. on behalf of Chinese Pharmaceutical Association and Institute of Materia Medica, Chinese Academy of Medical Sciences. This is an open access article under the CC BY-NC-ND license (http://creativecommons.org/licenses/by-nc-nd/4.0/).

Lysosome;
Mitochondria;
Mitophagy;
NRF2

present study, we showed that transcription factor EB (TFEB), a master transcription factor for lysosomal biogenesis, was impaired by APAP resulting in decreased lysosomal biogenesis in mouse livers. Genetic loss-of and gain-of function of hepatic TFEB exacerbated or protected against AILI, respectively. Mechanistically, overexpression of TFEB increased clearance of APAP protein adducts and mitochondria biogenesis as well as SQSTM1/p62-dependent non-canonical nuclear factor erythroid 2-related factor 2 (NRF2) activation to protect against AILI. We also performed an unbiased cell-based imaging high-throughput chemical screening on TFEB and identified a group of TFEB agonists. Among these agonists, salinomycin, an anticoccidial and antibacterial agent, activated TFEB and protected against AILI in mice. In conclusion, genetic and pharmacological activating TFEB may be a promising approach for protecting against AILI.

© 2024 The Authors. Published by Elsevier B.V. on behalf of Chinese Pharmaceutical Association and Institute of Materia Medica, Chinese Academy of Medical Sciences. This is an open access article under the CC BY-NC-ND license (http://creativecommons.org/licenses/by-nc-nd/4.0/).

1. Introduction

Acetaminophen (APAP) is a safe and effective drug at therapeutic doses, but an overdose can cause severe liver injury resulting in acute liver failure in animals and man[1]. APAP overdose is the most frequent cause of acute liver failure of any etiology in the US and many western countries[1−3]. The mouse model is clinically highly relevant to APAP-induced liver injury (AILI)[4], therefore the understanding of the pathophysiology of AILI in the mouse can have direct clinical impact on identifying novel therapeutic targets and intervention strategies[4]. Decades of studies into the mechanisms of APAP-induced liver injury have led to the enriched understanding of the formation of *N*-acetyl-*p*-benzoquinone imine (NAPQI) and subsequent APAP protein adducts in particular mitochondrial adducts, which triggers mitochondrial dysfunction and subsequent hepatocyte necrosis. Despite major progress in understanding mechanisms for APAP-induced liver injury, the only current FDA-approved treatment is to use *N*-acetylcysteine (NAC) that scavenges the reactive metabolites. However, the clinical use of NAC is often unsuccessful because NAC has very narrow therapeutic window and most patients in the clinic are already in the late phase of liver injury.

While convincing evidence supports the role of mitochondrial damage in APAP-induced necrosis, cells can respond to cellular stress and dysfunctional mitochondria by activating selective autophagy to remove damaged mitochondria[5−8]. Meanwhile, cells can also activate mitochondria biogenesis to replace the damaged mitochondria and maintain the homeostasis of mitochondria that provide sufficient ATP production, a process that is crucial for the liver repair and recovery of mice and humans from APAP intoxication[9]. We previously demonstrated that autophagy removes APAP adducts and damaged mitochondria to protect against APAP-induced liver injury after an overdose[6,10,11] and after multiple therapeutic doses[12]. We further showed that SQSTM1/p62, an autophagy receptor protein, is critical for selective removal of APAP-Adducts[11,13], supporting the notion that pharmacological activation of autophagy may be beneficial for treating AILI.

Autophagic degradation relies on the lysosome, which is the terminal component of autophagy that contains more than 50 acid hydrolases. During the induction of autophagy, increased lysosomal biogenesis is necessary to meet the need for the fusion with autophagosomes and subsequent autophagic degradation. The transcription regulation of lysosome biogenesis genes is mediated by the transcription factor EB (TFEB), which is a basic helix−loop−helix leucine zipper transcription factor belonging to the coordinated lysosomal expression and regulation (CLEAR) gene network[14]. Interestingly recent studies from others and ours indicate that TFEB also regulates mitochondrial biogenesis by directly regulating the expression of PGC-1α, a key transcription co-activator for mitochondrial biogenesis[15,16]. TFEB is mainly regulated at its posttranslational level. TFEB is phosphorylated at Ser142 by extracellular signal-regulated kinase 2 (ERK2) and at both Ser142 and Ser211 by mechanistic target of rapamycin complex 1 (mTORC1), which promotes TFEB binding with the cytosolic chaperone 14-3-3 and sequesters TFEB in the cytosol, resulting in its inactivation[14,17,18]. Conversely, the phosphatase calcineurin dephosphorylates TFEB at Ser142 and Ser211 and promotes TFEB nuclear translocation in response to lysosomal Ca^{2+} release[18]. Overexpression of TFEB using an adenovirus-TFEB increased expression of autophagy and lysosomal genes as well as PGC1α-mediated mitochondrial bioenergetics and protects against alcoholic and non-alcoholic liver disease and pancreatitis[16,19,20]. We previously demonstrated that pharmacological activation of autophagy by mTORC1 inhibitors, significantly reduces AILI in mice in co-treatment and post-treatment of APAP mouse model[10,11]. These published findings support the concept that autophagy plays an important role in defending against APAP-induced hepatotoxicity and offer protection against AILI even after APAP-induced hepatotoxicity is already initiated. However, in addition to regulating TFEB and autophagy, mTORC1 also regulate synthesis of proteins and lipids that are critical for cell proliferation. Indeed, mice with genetic deletion of mTOR show no protection against AILI due to impaired hepatocytes proliferation and liver regeneration[21]. Therefore, it is urgently needed to search for autophagy and TFEB activators independent of mTOR.

In the present study, we found that APAP treatment decreased hepatic levels of TFEB in mouse livers. Liver-specific deletion or overexpression of TFEB exacerbated or protected against AILI, respectively. We also established a cell-based imaging high throughput screening for TFEB agonists and identified a group of TFEB agonists. Among them, we showed that salinomycin, an anti-bacteria agent, activated TFEB and protected against AILI.

2. Materials and methods

2.1. Animal experiments

Tfeb Flox/Flox (*Tfeb*$^{flox/flox}$) mice were generated as described previously[16] and were crossed with Albumin Cre (Alb-Cre,

C57BL/6J, Jackson Laboratory) for at least nine generations to generate liver-specific *Tfeb* KO (*Tfeb*$^{flox/flox}$, Albumin-Cre+, L-*Tfeb* KO) mice. Alb-Cre- (*Tfeb*$^{flox/flox}$, Albumin-Cre-, WT) matched littermates were used in this study. All animals received humane care. Mice were specific pathogen free (SPF) and maintained in a barrier rodent facility under standard experimental conditions. All procedures were approved by the Institutional Animal Care and Use Committee of the University of Kansas Medical Center (Kansas City, KS, USA). Two to three-month-old male mice were used for all experiments. Briefly, mice were intraperitoneally injected with 500 mg/kg acetaminophen (APAP, Sigma−Aldrich, A5000) dissolved in warm saline or saline alone. Liver and serum samples were collected from mice after APAP overdose for 0.5, 2, 6 and 24 h. For overexpression of TFEB, wildtype mice were given one single dose of adenovirus of (Ad)-Null (5×10^8 PFU/mouse, intravenously [i.v.]) or Ad-TFEB (5×10^8 PFU/mouse, i.v.) for 10 days, before acetaminophen injection. Liver injury was determined by serum alanine aminotransferase (ALT) activity (Pointe Scientific, T7526-450). Male 2−3 month-old WT C57BL/6J mice were injected with acetaminophen (APAP, 500 mg/kg, i.p.) or saline for 6 and 24 h. Some mice were injected with salinomycin (5 mg/kg dissolved in 0.5% CMC-Na, i.p.) or equal volume of 0.5% CMC-Na (vehicle control) at the same time.

2.2. Cell culture and treatment

Primary mouse hepatocytes were isolated through two-step perfusion methods and cultured as previously described[11]. p62 knockout (KO) mice were described previously[22,23]. Control adenovirus (Ad-Null, 5 MOI) or adenovirus to overexpress TFEB (Ad-TFEB, 5 MOI) were added to William's medium E with 10% FCS, 1% L-glutamine and penicillim/streptomycin in WT and p62 KO hepatocyte. The cells were allowed for attachment for 2 h and changed to FBS free William's medium E. Total RNA was collected 24 h after adenovirus infection. In some experiments, hepatocytes were treated with APAP (10 mmol/L) in the presence or absence of chloroquine (CQ, 20 μmol/L) for 6 h. Some cells were further stained with tetramethylrhodamine methyl ester [TMRM, 50 nmol/L, Invitrogen (Carlsbad, CA)] and Hoechst 33342 [1 μg/mL, Invitrogen (Carlsbad, CA)] followed by fluorescence microscopy analysis for mitochondrial membrane potential changes. AML12 (ATCC, CRL-2554^{TM}) cells were maintained in DMEM/F-12 medium (HyClone, SH30271) supplemented with 10% FBS (Gibco), 1% L-glutamine and penicillin/streptomycin, 1 × ITS-X (insulin/transferrin/selenium, Gibco), and 40 ng/mL dexamethasone (Sigma−Aldrich, D2915) at 37 °C under 5% CO_2. When cells were incubated with salinomycin or torin 1, DMEM/F-12 medium supplemented with 10% FBS and 1% L-glutamine and penicillin/streptomycin was used. Stable expressing pEGFP-TFEB AML12 cell line was established and cultured as previously described[24]. Fluorescence images were acquired using a fluorescence microscope (Nikon Eclipse 200) with MetaMorph software.

2.3. Luciferase assay

TFEB promoter-driven luciferase reporter plasmid pGL3-TFEB-Luc was described previously[25]. AML12 cells were seeded in 48-well plate and transfected with pGL3-TFEB-Luc using Lipofectamine 2000 (Invitrogen, 11668019) according to manufacturer's instructions. After transfection for 24 h, cells were treated with salinomycin and Torin1 at indicated concentration for 24 h. TFEB-luciferase activity was determined using Luciferase Reporter Assay System (Promega, E1500) according to manufacturer's instructions. Relative firefly luciferase activity was normalized to protein concentration. Data are expressed as fold of control.

2.4. Histology and immunohistochemistry

Paraffin-embedded liver sections were stained with H&E and observed under a Nikon microscope. Terminal deoxynucleotidyl transferase dUTP nick and labeling (TUNEL) staining was performed in paraffin-embedded liver sections using the In Situ Cell Death Detection TUNEL Kit (Roche, 11684809910) according to manufacturer's instructions. Necrosis areas were estimated by scanning the entire tissue sections/slides from 3 mice in each group and presented as the percentage of the total liver section areas.

2.5. Immunofluorescence staining and confocal microscopy

Fresh mouse liver tissues were fixed in 4% paraformaldehyde overnight and then switched to 20% sucrose and stored at 4 °C for approximately 24 h. Liver tissues then were embedded in O.C.T. and stored at −20 °C. Five-μm sections were used for immunostaining with indicated primary antibodies followed by Alexa 488 or Rhodamine 123-conjugated secondary antibody. The LAMP1 antibody was from Developmental Studies Hybridoma Bank (1D4B). Secondary antibodies were from Jackson ImmunoRe search. Confocal images were obtained using a Leica TCS SPE confocal microscope (DM550 Q).

2.6. Electron microscopy

Liver tissues were cut into small pieces and fixed in 2% glutaraldehyde in 0.1 mol/L phosphate buffer (pH 7.4), followed by 1% OsO_4. After dehydration, thin sections were cut and stained with uranyl acetate and lead citrate. Digital images were captured using a JEM 1016CX electron microscope. Random images were selected from around 20 different cells, and the number of typical autophagosomes that enveloped with mitochondria from each cell section was counted.

2.7. Cellular fractionation and Western blot analysis

Total liver lysates were prepared using radioimmunoprecipitation assay (RIPA) buffer (1% NP40, 0.5% sodium deoxycholate, 0.1% sodium dodecyl (lauryl) sulfate). Nuclear and cytoplasmic fractions of liver tissue were prepared by using a commercial kit (Thermo scientific, 78835). Protein (30 μg) was separated by a 12% SDS-PAGE gel before transfer to a PVDF membrane. Membranes were probed using appropriate primary and secondary antibodies and developed with SuperSignal West Pico chemiluminescent substrate (Life Technologies, 34080). The following antibodies were used for Western blot analysis: TFEB (Bethyl Laboratories, A303-673A), CYP2E1 (Abcam, Ab789013), Lamp1 (Developmental Studies Hybridoma Bank, 1D4B), phosphor-JNK (Cell Signaling Technology, 9255), total-JNK (Cell Signaling Technology, 9252), LC3B (Cell Signaling Technology, 3868), OXPHOS cocktail (Abcam, ab110413), p62/SQSTM1 (Abnova, H00008878-M01), TFAM (Abcam, ab252432), β-actin (Sigma−Aldrich, a5541), GAPDH (Cell Signaling Technology, 2118), Lamin A/C (Cell Signaling

Technology, 2032). VATP6V1A and VATP6V1B2 antibodies were gifts from Dr. Dennis Brown from Harvard Medical School. Glutamate-Cysteine Ligase Catalytic Subunit (GCLC) and Glutamate-Cysteine Ligase Modifier Subunit (GCLM) antibodies were gifts from Dr. Terry Kavanagh from the University of Washington. The APAP-adduct antibody was a gift from Dr. Lance Pohl from NIH as we described previously[11]. Secondary antibodies conjugated to horseradish peroxidase were from Jackson ImmunoResearch. The results were analyzed by ImageJ.

2.8. RNA extraction and real-time q-PCR

Total RNAs from mouse livers, isolated mouse primary hepatocytes and cultured cells were isolated by using TRIzol reagent (Thermo Fisher Scientific, 15596-026) and GeneJET RNA Purification Kit (Thermo Fisher Scientific, K0732), respectively, and were reverse-transcribed into cDNA using RevertAid Reverse Transcriptase (Thermo Fisher Scientific, EP0442). Quantitative polymerase chain reaction (qPCR) was performed using SYBR Green chemistry (Bio-Rad, 1725124). Primer sequences (5′−3′) used in qPCR are listed in Table 1. Real-time qPCR results were normalized to 18s. Data are expressed as fold of control.

2.9. Glutathione (GSH) assay

Hepatic GSH levels in mouse livers were determined using Glutathione Colorimetric Assay Kit (BioVision, K261) according to manufacturer's instructions. Briefly, approximately 50 mg liver tissues were homogenized in sulfosalicylic acid (1%) and centrifuged at 8000 × *g* for 10 min. Supernatant was collected and subjected to a cycling reaction using GSH reductase and GSH substrate dithionitrobenzoic acid (DTNB), and GSH levels were determined by spectrophotometry at 412 nm.

2.10. Cathepsin B activity

Cathepsin B activity was determined using mouse liver lysates. The liver tissues were lysed in ice-cold lysis buffer (50 mmol/L Tris (pH 7.4), 130 mmol/L NaCl, 10% glycerol, 0.5% NP-40, 0.5 mmol/L EDTA, and 0.5 mmol/L EGTA). After centrifugation, total protein concentration was calculated and then 15 μg protein from each sample was added to assay buffer (10 mmol/L HEPES-NaOH (pH 7.4), 220 mmol/L mannitol, 68 mmol/L sucrose, 2 mmol/L NaCl, 2.5 mmol/L KH_2PO_4, 0.5 mmol/L EGTA, 2 mmol/L $MgCl_2$, 5 mmol/L pyruvate, and 1 mmol/L dithiothreitol). The enzyme activity was determined by adding cathepsin B substrate *Z*-Arg-Arg-AMC (Calbiochem, 219392) and measured at 355 nm/460 nm. Data are expressed as fold of control.

2.11. GFP-TFEB nuclear translocation assay in a quantitative high throughput screening (qHTS) format

AML-12-pEGFP-N1-TFEB (GFP-TFEB) cells suspended in assay medium (1:1 mixture of Dulbecco's modified Eagle's medium and Ham's F12 medium with 10% FBS and 1% P/S) were dispensed at 1000 cells/5 μL/well in PDL coated low-base clear bottom/black wall 1536-well plates using a Flying Reagent Dispenser (FRD, Aurora Discovery, San Diego, CA, USA). After the assay plates were incubated at 37 °C/5% CO_2 for 18 h, 23 nL of a test compound dissolved in dimethylsulfoxide (DMSO), positive control (Torin 1, Tocris Bioscience), or vehicle control (DMSO), was transferred to the assay plates using a Wako Pintool station (Wako Automation, San Diego, CA, USA). The final compound concentration in the assay well ranged from 0.8 nmol/L to 46 μmol/L over 11 concentrations. The assay plates were incubated at 37 °C/5% CO_2 for 2 h, and then 5 μL of premixed fix and stain solution

Table 1 List of mouse primers used for qPCR.

Gene	Forward primer (5′−3′)	Reverse primer (5′−3′)
18s	TAGAGGGACAAGTGGCGTTC	CGATGAGCCAGTCAGTGT
Atg5	GACCACAAGCAGCTCTGGAT	GGTTTCCAGCATTGGCTCTA
Atg8	CCGAGAAGACCTTCAAGCAG	ACACTTCGGAGATGGGAGTG
Cyp2E1	TGGTGGAGGAGCTCAAAAAG	GTGTTCCTTGGCTTTTCCAA
Gclc	AACACAGACCCAACCCAGAG	CCGCATCTTCTGGAAATGTT
Gclm	TGTGTGATGCCACCAGATTT	GATGATTCCCCTGCTCTTCA
Gsr	TCCAAGTGGTGACTTCCGTG	CATCCGTCTGAATGCCCACT
Keap1	AAGGAACATGATATGCCCTGACA	ACACAGGCCGGCTCCAT
Lamp1	AGCATACCGGTGTGTCAGTG	GTTGGGGAAGGTCCATCCTG
Lamp2	TGCAGTGCAGATGAAGACAAC	GCTATGGGCACAAGGAAGTTG
Mfn2	AGGGCTCGGAGAAGGTATGT	CTCAGTGGCAAGAAGGGAGG
MnSOD	GGCCAAGGGAGATGTTACAA	AGACACGGCTGTCAGCTTCT
Nqo1	CAGATCCTGGAAGGATGGAA	TCTGGTTGTCAGCTGGAATG
Nrf2	CGAGATATACGCAGGAGAGGTAAGA	GCTCGACAATGTTCTCCAGCTT
Sqstm1/p62	AGAATGTGGGGGAGAGTGTG	TCGTCTCCTCCTGAGCAGTT
Pgc1α	ATGTGTCGCCTTCTTGCTCT	ATCTACTGCCTGGGGACCTT
Ppar-α	ATGCCAGTACTGCCGTTTTC	GGCCTTGACCTTGTTCATGT
Ppar-γ	TTTTCAAGGGTGCCAGTTTC	AATCCTTGGCCCTCTGAGAT
TFAM	AAGGGAATGGGAAAGGTAGA	AACAGGACATGGAAAGCAGAT
Tfeb	CCAGAAGCGAGAGCTCACAGAT	TGTGATTGTCTTTCTTCTGCCG
Tfe3	CCTGAAGGCATCTGTGGATT	CTCGTGGTTAGGGAGAGCAG
Tom20	TGCCCATTTTAGGACCCACC	CCAGCCTTGACGTCTTCCTT
Vatp6v1d	GAGCACAGACTGGTCGAAA	AGCTGTCAGTTCCTTCGTGG
Vatp6v1h	ATGAGTACCGGTTTGCCTGG	GACTGAATGCCAGGAGCCAT
Vatp6v0e1	ATACCACGGCCTTACTGTGC	CAGAGGATTGAGCTGTGCCA

containing 8% PFA with 0.1% Hoechst (final concentration, 4% PFA with 0.05% Hoechst) was added on top of each well of the assay plates by FRD. After the assay plates were left at RT for 30 min, the medium with fix solution was removed by gentle-spin of Blue-Washer (Blue Cat Bio, Concord, MA, USA), followed by adding HBSS (9 μL/well) by FRD. Image from each assay well was acquired using 20 × water, confocal objective lenses in PerkinElmer Operetta CLS with EGFP channel (Excitation 460−490 nm, Emission 500−550 nm) and DAPI (Excitation 355−385 nm, Emission 430−500 nm) filter sets. Images from each well were acquired for one center field (around 25% of a single well area in a 1536-well plate) and analyzed with software of Operetta Harmony 4.6. Data analysis was performed as previously described[26]. Briefly, raw plate reads for each titration point were first normalized to the Torin 1 control (1.15 μmol/L, 100%) and DMSO-only wells (basal, 0%) and then corrected by applying a pattern correction algorithm. Concentration−response titration points for each compound were fitted to the Hill equation, yielding concentrations of half-maximal induction (EC_{50}) and maximal response (efficacy) values.

2.12. *Statistical analysis*

All experimental data are expressed as mean ± standard error (SE). One-way ANOVA with Bonferroni *post hoc* test or Student's *t*-test was performed where appropriate. A $P < 0.05$ was considered significant.

3. Results

3.1. *APAP overdose impairs TFEB in mouse livers*

To determine whether APAP overdose would affect hepatic levels and transcription activity of TFEB, mice were treated with 500 mg/kg APAP for 6 and 24 h. Compared with mice injected with saline, the levels of serum alanine aminotransferase (ALT) significantly increased after APAP treatment for 6 or 24 h (Fig. 1A). Immunoblot analysis showed that APAP treatment significantly decreased the protein levels of TFEB in total liver lysates, cytosolic and nuclear fractions (Fig. 1B and C). Moreover, the protein levels of VATP6V1A and VATP6V1B2, two subunits

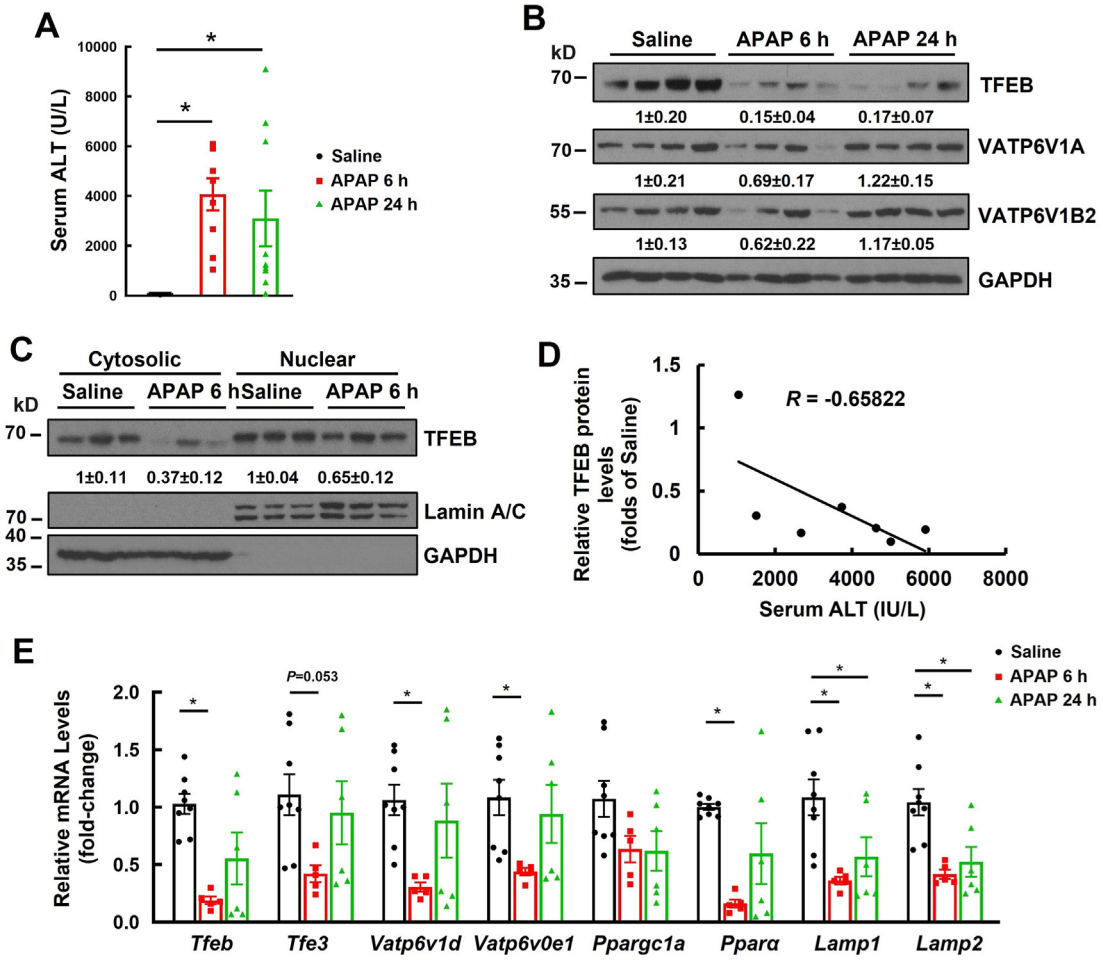

Figure 1 APAP overdose reduces TFEB activity in mouse livers. Male C57BL/6J wildtype (WT) mice were injected with acetaminophen (APAP, 500 mg/kg, i.p.) or saline for 6 or 24 h. (A) Serum ALT levels were quantified. Data are mean ± SE ($n = 9-10$); *$P < 0.05$; One-way ANOVA analysis. (B) Total liver lysates were subjected to Western blot analysis. (C) Cytosolic and nuclear fractions from mouse livers were subjected to Western blot analysis. (D) A scatter plot and linear regression analysis of expression levels of serum ALT levels *vs.* hepatic TFEB protein levels in WT mice injected with APAP (500 mg/kg) for 6 h. (E) Hepatic mRNA was extracted followed by qPCR. Results were normalized to 18s and expressed as fold change compared to Saline group. Data are mean ± SE ($n = 4-8$); *$P < 0.05$; One-way ANOVA analysis.

of lysosomal v-ATPase, also decreased at 6 h after APAP treatment (Fig. 1B). Interestingly, the protein levels of TFEB were negatively correlated with the serum ALT levels in APAP-treated mice (Fig. 1D). The mRNA levels of TFEB targeted genes, including *Tfeb*, *Tfe3*, *Ppargc1a*, *Ppara*, *Lamp1*, *Lamp2*, *Vatp6v1d* and *Vatp6v0e1*, were significantly lower in mice treated with APAP for 6 h than the saline-treated mice, although the mRNA levels of most genes were recovered after APAP treatment for 24 h (Fig. 1E). Taken together, these data indicate that APAP overdose impairs TFEB function in mouse livers.

3.2. *Loss of hepatic TFEB exacerbates APAP-induced liver injury (AILI) in mice*

To determine whether the decreased hepatic TFEB would contribute to AILI in mice, liver-specific *Tfeb* knockout (L-*Tfeb* KO) and matched wildtype (WT) mice were subjected to APAP overdose. The levels of serum ALT activities were increased 1.5-fold in L-*Tfeb* KO mice compared with the matched WT mice after APAP treatment for 6 h. However, the levels of serum ALT activities were almost identical between L-*Tfeb* KO and WT mice after APAP treatment for 24 h (Fig. 2A). The necrotic areas in L-*Tfeb* KO mouse livers were much higher than WT mice after APAP treatment for both 6 and 24 h, indicating loss of hepatic *Tfeb* exacerbates APAP-induced hepatotoxicity (Fig. 2B−D). To determine if deletion of *Tfeb* would affect the metabolism of APAP in mouse livers, levels of hepatic CYP2E1, glutathione (GSH) and APAP-adducts were examined in WT and L-*Tfeb* KO mice following APAP treatment. Levels of hepatic CYP2E1 were increased almost 2-fold in APAP-treated WT mouse livers compared with saline-treated control WT mice. Interestingly, the basal levels of hepatic CYP2E1 in L-*Tfeb* KO mice were higher (2.3-fold) than the matched WT mice but APAP treatment did not further alter the levels of CYP2E1 in L-*Tfeb* KO mice (Fig. 2E). APAP markedly increased levels of phosphorylated JNK in APAP-treated WT mouse livers. In the APAP-treated L-*Tfeb* KO mice, there were varying levels of phosphorylated JNK. Two of the mice had lower levels, but two had similar levels of phosphorylated TFEB compared to the APAP-treated WT mice. The levels of hepatic APAP-adducts were slightly lower (decreased 30%) in APAP-treated L-*Tfeb* KO than WT mice (Fig. 2E). Furthermore, the levels of hepatic GSH were significantly decreased after APAP treatment at 0.5, 2 and 6 h but recovered at 24 h to the similar level in both WT and L-*Tfeb* KO mice (Fig. 2F), suggesting that deletion of *Tfeb* may not affect the metabolism of APAP. Taken together, loss of hepatic TFEB does not alter APAP bioactivation but exacerbates AILI.

3.3. *Overexpression of TFEB protects against AILI in mice*

To further determine the role of TFEB in AILI, we next overexpressed TFEB in mouse livers by i.v. injection of an adenovirus-*Tfeb* (Ad-*Tfeb*) in WT mice. Ad-TFEB administration dramatically increased the protein and mRNA levels of TFEB in mouse livers, indicating successful overexpression of TFEB in mouse livers (Fig. 3A and B). Overexpression of TFEB almost completely abolished AILI as demonstrated by the markedly decreased levels of serum ALT and AST as well as necrotic areas of H&E staining and TUNEL positive staining (Fig. 3C−E). Overexpression of TFEB slightly increased hepatic levels of CYP2E1 to 37% compared to mice receiving the adenovirus vector only in saline-treated mice. However, overexpression of TFEB did not cause a further increase of hepatic levels CYP2E1 in APAP-treated mice (Fig. 3F). Moreover, overexpression of TFEB markedly decreased the levels of both liver and serum APAP-adducts in APAP-treated mice (Fig. 3F and G). Notably, the expression level of TFEB was relatively lower in one mouse after receiving Ad-*Tfeb* (dot-line boxed) likely due to insufficient i.v. injection, which was correlated with relatively higher levels of liver and serum APAP-adducts after APAP treatment (Fig. 3F and G). These data indicate that overexpression of TFEB protects against AILI likely *via* increased clearance of APAP-adducts in mice.

3.4. *Overexpression of TFEB increases lysosomal and autophagy-related gene expression in mouse livers*

Overexpression TFEB significantly increased protein levels of LAMP1, p62, VATP6V1A, and LC3-II (Fig. 4A). Moreover, overexpression of TFEB also significantly increased the activity of cathepsin B without or without APAP treatment, suggesting possible increased lysosome contents and autophagic degradation (Fig. 4B). Overexpression of TFEB also showed a trend of increased expression of several autophagy-related genes and lysosomal genes including *Sqstm1*, *Atg5*, *Atg8*, *Lamp1*, *Vatp6v1d*, *Vatp6v0e1* and *Vatp6v1h* with or without APAP treatment (Fig. 4C). The number of lysosomes, as demonstrated by the positive LAMP1 puncta, decreased in hepatocytes of APAP-treated mice but were markedly recovered by TFEB overexpression (Fig. 4D and E). Collectively, these data indicate that overexpression of TFEB increases hepatic lysosomal numbers and autophagy activity, which may promote the removal of APAP-adducts.

3.5. *Overexpression of TFEB activates NRF2 pathway in mouse livers and primary hepatocytes*

Overexpression of TFEB markedly increased the protein levels of GCLC and GCLM, two NRF2 targeted genes and subunits of GSH synthesis in mouse livers with or without APAP treatment (Fig. 5A). Overexpression of TFEB also increased the mRNA levels of *Keap1*, *Nfe2l2*, and NRF2 targeted genes *Gclc*, *Gclm*, *Nqo1* and *Gsr* in saline treated mice but at a lesser extent in APAP-treated mice (Fig. 5B). Intriguingly, results from the cellular fractionation analysis revealed that overexpression of TFEB did not increase nuclear NRF2 levels (Fig. 5C). Since p62 can activate NRF2 *via* the non-canonic pathway by binding with KEAP1, we next asked whether p62 is involved in increased NRF2 activation in mouse livers with TFEB overexpression. We found that overexpression of TFEB significantly increased the mRNA levels of *Sqstm1* and NRF2 targeted genes *Gclc* and *Gclm* in hepatocytes isolated from WT mice (Fig. 5D). Interestingly, while the mRNA levels of *Tfeb* was almost identical in WT and p62 KO hepatocytes infected with Ad-*Tfeb*, increased mRNA levels of *Gclc* and *Gclm* in WT hepatocytes infected with Ad-*Tfeb* were abolished in p62 KO hepatocytes (Fig. 5D). These data indicate that overexpression of TFEB may activate KEAP1−NRF2 pathway in hepatocytes indirectly *via* p62-mediated non-canonical NRF2 activation. Consistent with induction of *Gclc* and *Gclm* in TFEB overexpressed mouse livers, there was a faster recovery of hepatic GSH levels (Fig. 5E), which could

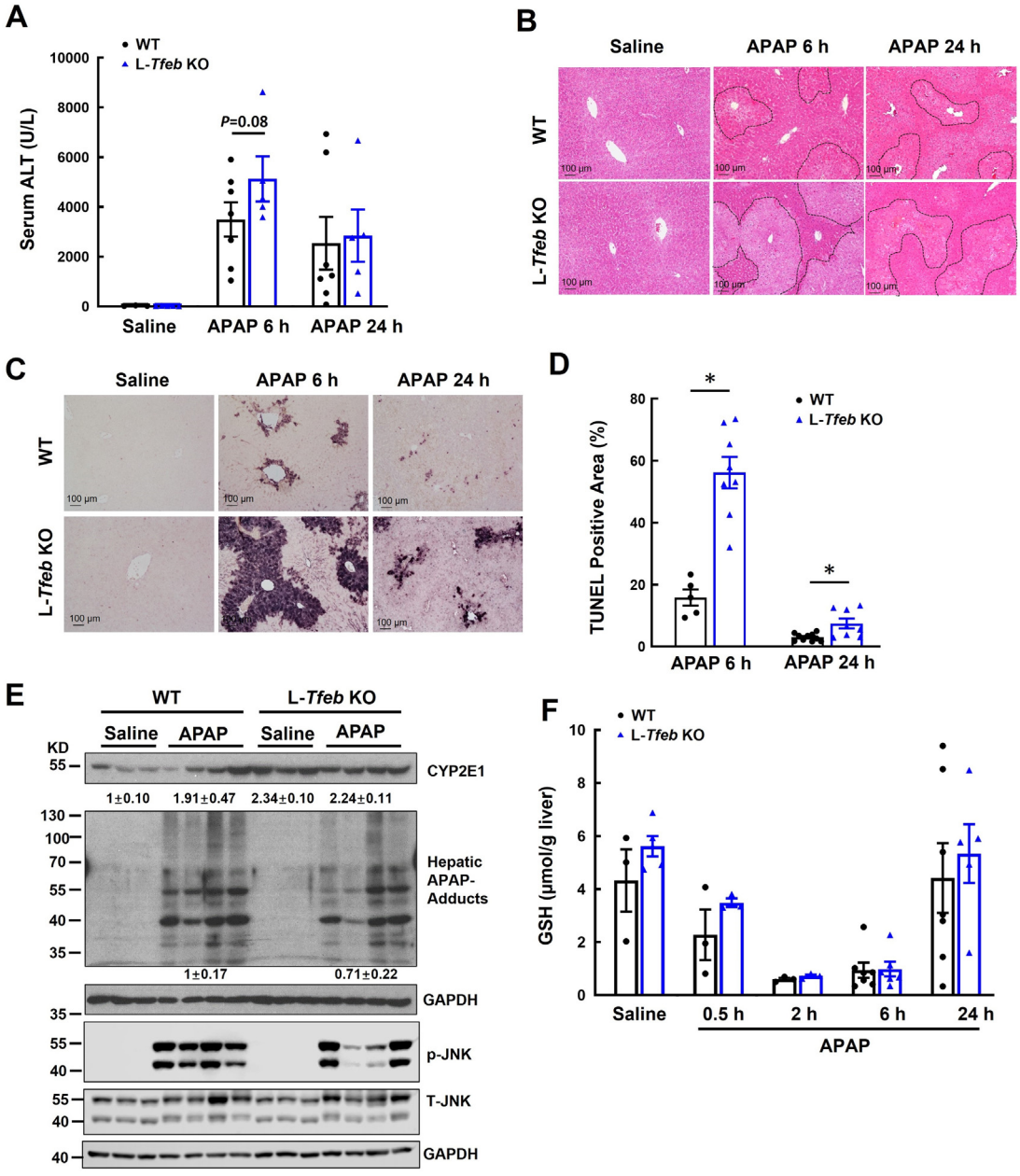

Figure 2 Hepatic loss of TFEB exacerbates APAP overdose-induce liver injury in mice. Male liver-specific *Tfeb* KO (*Tfeb*$^{flox/flox}$, Albumin-Cre+, L-*Tfeb* KO) mice and their matched WT mice (*Tfeb*$^{flox/flox}$, Albumin-Cre-, WT) were injected with APAP (500 mg/kg, i.p.) for 6 and 24 h. (A) Serum ALT levels were quantified. Data are mean ± SE (n = 3−7). (B) Representative images of H&E staining are shown (magnification 100 ×). (C) Representative images of TUNEL staining are shown (magnification 100 ×). (D) Quantification of TUNEL positive areas from TUNEL staining of (C). Data are mean ± SE (n = 3). *$P < 0.05$; One-way ANOVA analysis. (E) Total liver lysates were subjected to Western blot analysis. (F) Total hepatic glutathione (GSH) contents were determined. Data are mean ± SE (n = 3−7).

be a contributing factor to the protection against APAP overdose in these animals.

3.6. *Overexpression of TFEB increases mitochondria biogenesis and mitophagy in mouse livers*

We previously demonstrated that TFEB overexpression increased mitochondrial bioenergetics and mitochondria respiration in mouse livers[19]. *Ppargc1a*, a TFEB target gene, played an important role in mitochondrial biogenesis, and overexpression of TFEB in muscular cells increased mitochondrial biogenesis[27]. We found that TFEB overexpression increased both protein and mRNA levels of TFAM and PGC1α, the mitochondrial transcription factor or co-activator, as well as two mitochondrial inner membrane proteins of mitochondria oxidative phosphorylation complexes [complexes I & V (CI & CV)] in mouse livers (Fig. 6A and B). More importantly, the expression levels of several genes that encoded mitochondrial proteins (*Mfn1, Mfn2, Tom20, Mnsod*) and lipid metabolism genes (*Ppara, Pparγ*) were also significantly increased in Ad-*Tfeb*

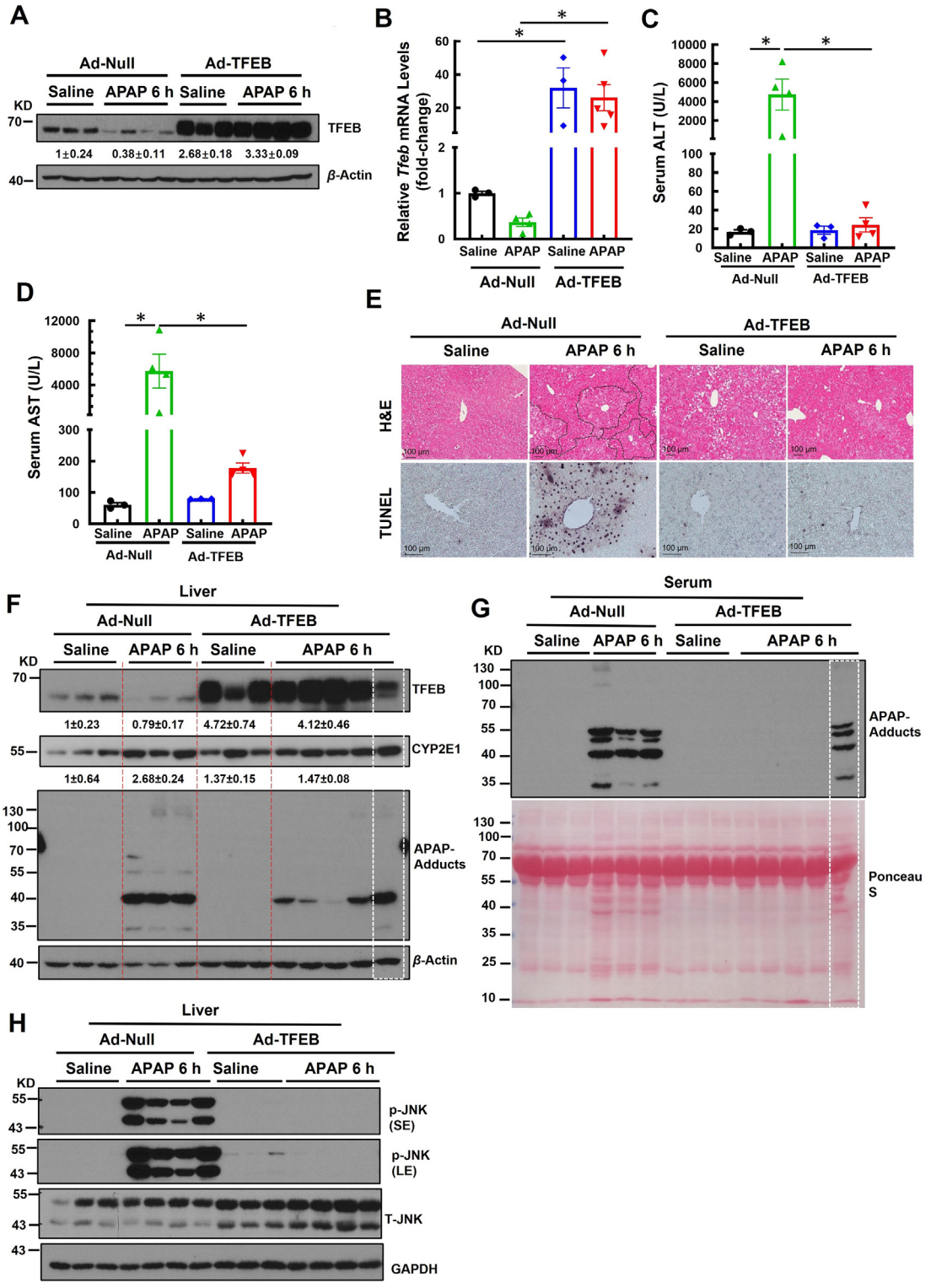

Figure 3 Overexpression of TFEB protects against APAP overdose-induced liver injury in mice. Male WT C57BL/6J mice were injected with Ad-Null and Ad-TFEB (5×10^8 PFU/mouse, i.v.) for 10 days followed by APAP injection (500 mg/kg, i.p.) for 6 h. (A) Total liver lysates were subjected to Western blot analysis. (B) Hepatic mRNA was extracted followed by qPCR. Results were normalized to 18s and expressed as fold change compared to Ad-Null + Saline group. Data are mean ± SE ($n = 3-4$). *$P < 0.05$; One-way ANOVA analysis. (C) Serum ALT and (D) AST levels were quantified. Data are mean ± SE ($n = 3-4$). *$P < 0.05$; One-way ANOVA analysis. (E) Representative images of H&E and TUNEL staining are shown (magnification 100 ×). (F) Total liver lysates were subjected to Western blot analysis. (G) Serums were subjected to Western blot analysis. (H) Total liver lysates were subjected to Western blot analysis for JNK activation.

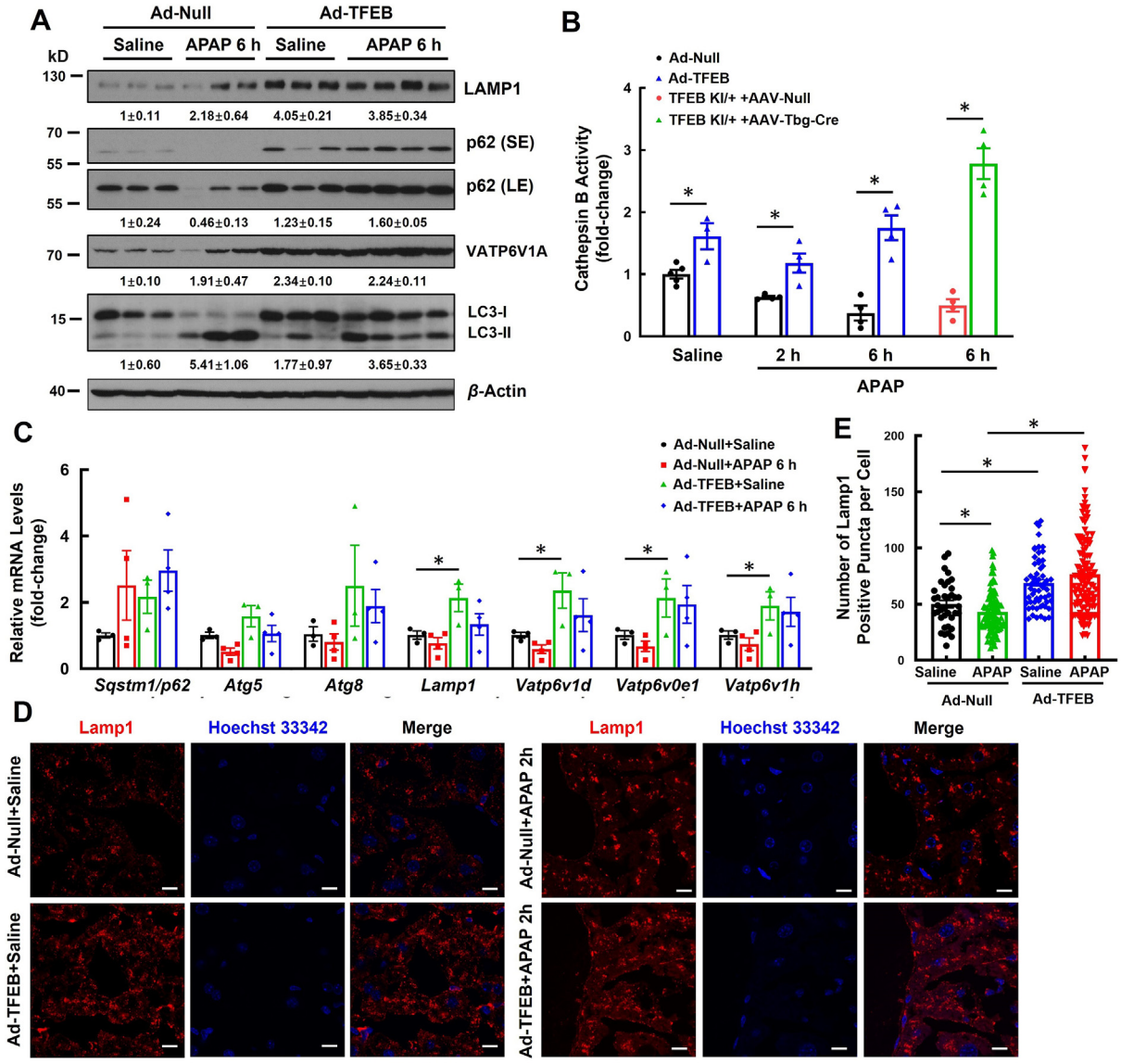

Figure 4 Overexpression of TFEB increased lysosomal and autophagic gene expression in mouse livers. Male WT C57BL/6J mice were injected with Ad-Null and Ad-TFEB (5×10^8 PFU/mouse, i.v.) for 10 days followed by APAP injection (500 mg/kg, i.p.) for 2 and 6 h. *Tfeb* knockin (KI) mice were injected with AAV-Null and AAV-Tbg-Cre (5×10^9 GC/mouse, i.v.) for 2 weeks followed by APAP injection (500 mg/kg, i.p.) for 6 h. (A) Total liver lysates were subjected to Western blot analysis. (B) Cathepsin B activities were determined. Data are mean ± SE ($n = 3-4$). *$P < 0.05$; One-way ANOVA analysis. (C) Hepatic mRNA was extracted followed by qPCR. Results were normalized to 18s and expressed as fold change compared to Ad-Null + Saline group. Data are mean ± SE ($n = 3-4$). *$P < 0.05$; One-way ANOVA analysis. (D) Representative images of immunostaining of Lamp1 are shown. Scale: 10 μm. (E) The quantified number of Lamp1 positive vesicles is shown. Data are mean ± SE ($n = 3-4$). 30 to 110 cells were counted in each mouse.

administrated mouse livers (Fig. 6B), suggesting TFEB overexpression may increase mitochondrial biogenesis in mouse livers. EM analysis revealed no apparent alterations in the quantity and dimensions of mitochondria in hepatocytes that had undergone TFEB overexpression, in comparison to mice that received Ad-null. However, treatment with APAP seemed to lead to an augment in mitophagy structures (which are mitochondria enclosed within double-membrane autophagosomes, as indicated by the arrows in Fig. 6C), with a notable rise in the number of those structures found in hepatocytes that had undergone TFEB overexpression (Fig. 6C and D). Together, these data indicate that overexpression of TFEB increases mitochondrial biogenesis and mitophagy in APAP-treated mouse livers.

3.7. Overexpression of TFEB increases autophagic flux and may protect against the loss of mitochondrial membrane potential in APAP-treated mouse hepatocytes

We next determined whether overexpression of TFEB would increase autophagic flux in APAP-treated hepatocytes by examining the changes in endogenous LC3-II in the presence of lysosomal inhibitor chloroquine (CQ)[28]. APAP treatment alone decreased the

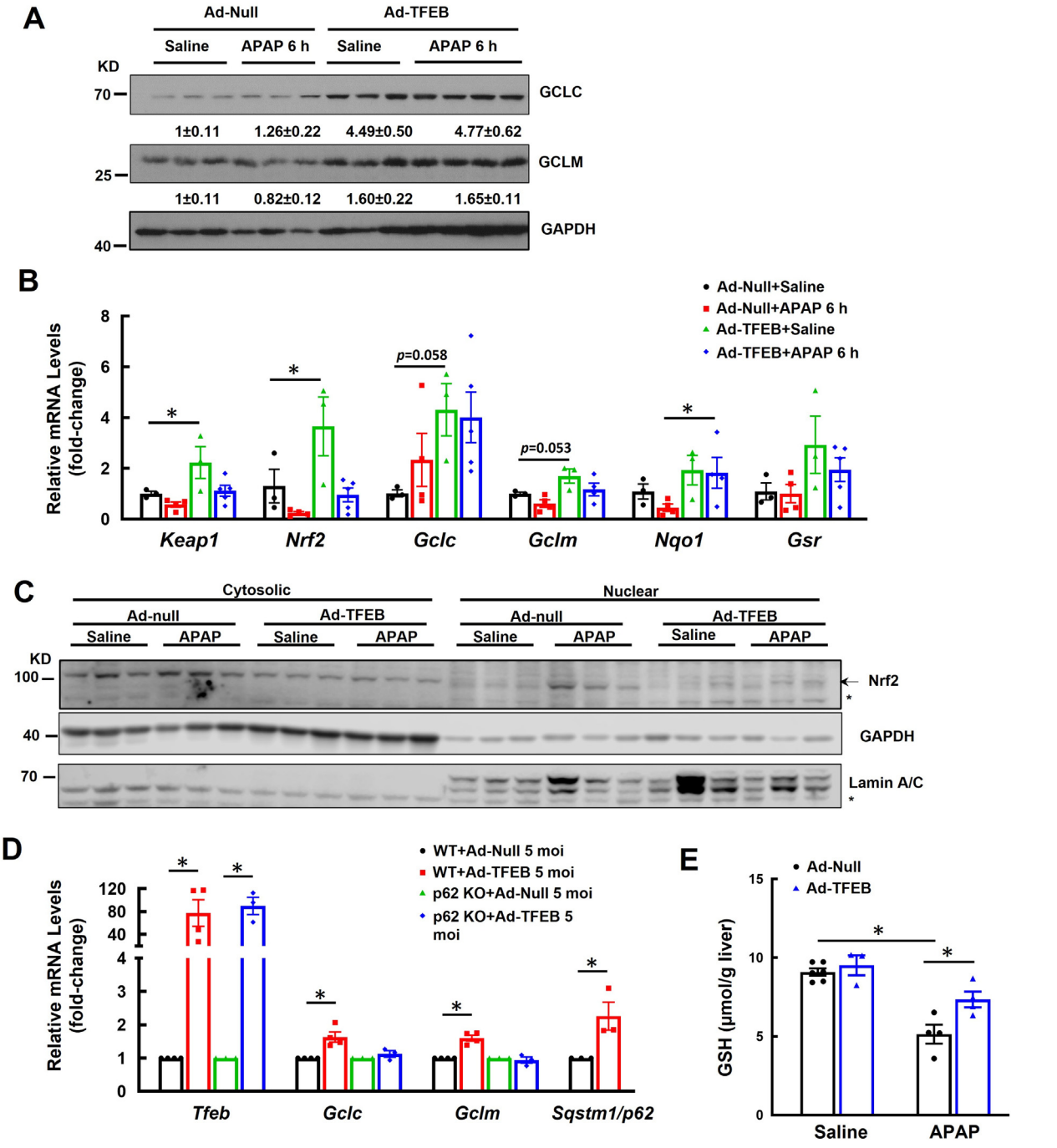

Figure 5 Overexpression of TFEB activates NRF2 pathway in mouse livers. Male WT C57BL/6J mice were injected with Ad-Null and Ad-TFEB (5×10^8 PFU/mouse, i.v.) for 10 days followed by APAP injection (500 mg/kg, i.p.) for 6 h. (A) Total liver lysates were subjected to Western blot analysis. (B) Hepatic mRNA was extracted followed by qPCR. Results were normalized to 18s and expressed as fold change compared to Ad-Null + Saline group. Data are mean ± SE ($n = 3-4$). *$P < 0.05$; One-way ANOVA analysis. (C) Cytosolic and nuclear fractions from the mouse livers of indicated treatments were subjected to Western blot analysis. (D) Primary mouse hepatocytes were isolated from wildtype and p62 KO mice and infected with Ad-Null and Ad-TFEB (5 moi) for 24 h. Total mRNAs were extracted followed by qPCR. Results were normalized to 18s and expressed as fold change compared to Ad-Null group. Data are mean ± SE ($n = 3-4$). *$P < 0.05$; One-way ANOVA analysis. (E) Male WT C57BL/6J mice were injected with Ad-Null and Ad-TFEB (5×10^8 PFU/mouse, i.v.) for 10 days followed by APAP injection (500 mg/kg, i.p.) for 6 h. Hepatic GSH contents were quantified. Data are mean ± SE ($n = 4-6$), *$P < 0.05$; One-way ANOVA analysis.

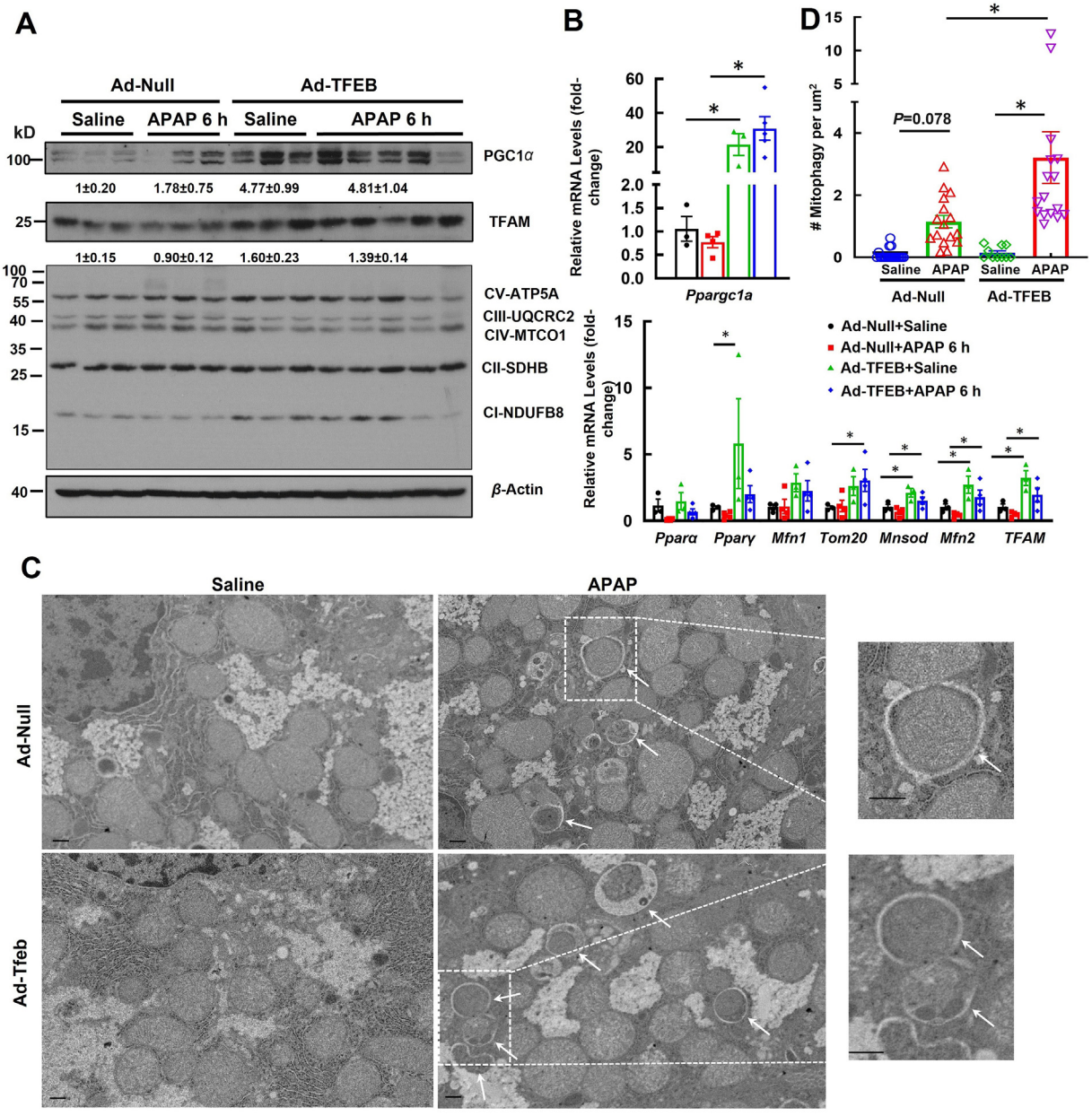

Figure 6 Overexpression of TFEB increases mitochondrial biogenesis in mouse livers. Male WT C57BL/6J mice were injected with Ad-Null and Ad-TFEB (5×10^8 PFU/mouse, i.v.) for 10 days followed by APAP injection (500 mg/kg, i.p.) for 6 h. (A) Total liver lysates were subjected to Western blot analysis. (B) Hepatic mRNA was extracted followed by qPCR. Results were normalized to 18 s and expressed as fold change compared to Ad-Null + Saline group. Data are mean ± SE ($n = 3-4$). *$P < 0.05$; One-way ANOVA analysis. (C) Liver tissues were fixed for EM analysis and representative EM images are shown. Arrows denote mitophagy structures (enveloped mitochondria in autophagosomes). Scale: 500 nm. (D) The number of mitophagy structures was quantified from each cell section of around 20 different cells. Data are mean ± SE ($n = 16-19$). *$P < 0.05$; One-way ANOVA analysis.

levels of LC3-II and p62, which may be due to increased autophagic degradation. However, this effect was partially rescued by CQ treatment regardless of TFEB expression level (Fig. 7A). In addition, when TFEB was overexpressed, the levels of LC3-II increased after CQ treatment as compared to hepatocytes that received Ad-null (Fig. 7A). This suggests that overexpression of TFEB may lead to an increase in autophagic flux in hepatocytes. Furthermore, APAP treatment resulted in an increase in the number of hepatocytes with depolarized mitochondria. However, this effect was partially reversed when TFEB was overexpressed as seen in Fig. 7B–D. This indicates that overexpression of TFEB may increase hepatic autophagy and help maintain proper mitochondrial functions in hepatocytes.

3.8. Identification of small molecules that activate TFEB and increases autophagic flux in AML12 cells using a qHTS platform

Since we found that overexpression TFEB protects against AILI in mice, we next established a mouse hepatocyte cell line stably expressing GFP-TFEB and performed a cell-based image assay

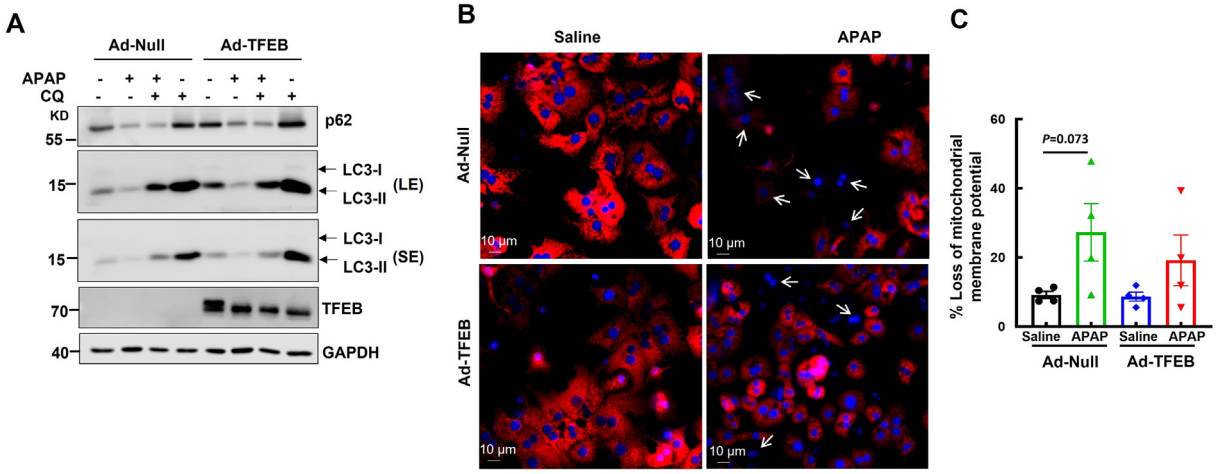

Figure 7 Overexpression of TFEB Increases autophagic flux and protects against the loss of mitochondrial membrane potential in APAP-treated mouse hepatocytes. Primary mouse hepatocytes were isolated from wild-type mice and infected with Ad-Null and Ad-TFEB (1 moi) for 24 h. Hepatocytes were then treated with APAP (10 mmol/L) in the presence or absence of chloroquine (CQ, 20 μmol/L) for 6 h. Total lysates were subjected to Western blot analysis (A). Some hepatocytes were cultured in 12-well plates and were further stained with TMRM (50 nmol/L) and Hoechst 33342 (1 μg/mL) followed by fluorescence microscopy and representative images are shown in (B, arrows denote cells with loss of mitochondrial membrane potential). (C) The number of cells with loss of TMRM staining (partial or complete loss of TMRM staining) was quantified, and the percentage of cells with loss of TMRM staining was calculated based on the total cell numbers in each field (based on Hoechst 33342 nuclei or phase-contrast images). Data are mean ± SE ($n = 4$) followed by One-way ANOVA analysis.

for screening TFEB agonists in a qHTS format. To identify the compounds that increase nuclear translocation of GFP-TFEB, GFP-TFEB stable AML12 cells were used to screen a group of 384 known anticancer compounds at 11 concentrations ranging from 0.8 nmol/L to 46 μmol/L. GFP-TFEB nuclear localization was quantified from GFP-TFEB AML12 cells that were treated with different concentrations of compound. A flowchart of the qHTS is shown in Fig. 8A. Torin 1 is known to increase TFEB nuclear translocation by inhibiting mTORC1, which was used as a positive control in the qHTS. Representative images of the qHTS and GFP-TFEB imaging analysis of control cells (DMSO) and Torin 1-treated cells were shown in Fig. 8B. The primary screening resulted in the identification of 137 compounds that had efficacy >40% and led to significant increase in GFP-TFEB nuclear translocation. Potential TFEB agonists that with EC_{50} less than 10 μmol/L were listed in Table 2.

Among these positive hits of TFEB agonists, sunitinib malate, an indolinone-based tyrosine kinase inhibitor, as well as daunorubicin and idarubicin hydrochloride, anthracycline antibiotics for treating acute myeloid leukemia, had as low as less than 2 μmol/L AC_{50} for TFEB activation (Table 2). Sunitinib has a dual role in AILI exhibiting mild hepatoprotective effect at low dose or increases AILI at high dose[29], whereas anthracycline antibiotics have increased cardiac and hepatic toxicity[30]. Salinomycin, an anticoccidial and antibacterial agent, also showed relatively high efficacy with an EC_{50} at 2.64 μmol/L (Table 2). We thus focused on salinomycin and first validated the effects of salinomycin on TFEB activation in cultured AML12 cells. While GFP-TFEB signals were diffuse in the cytoplasm of control AML12 cells, salinomycin and Torin1 significantly increased the nuclear translocation of TFEB (Fig. 8C). Moreover, using a luciferase reporter gene assay, salinomycin significantly increased the TFEB promoter driven luciferase activity, indicating that salinomycin may increase the transcription activity of TFEB in AML12 cells (Fig. 8D). Salinomycin treatment increased the mRNA levels of several TFEB target genes including *Tfeb*, *Sqstm1*, *Ppargc1a*, *Lamp1*, *Vatp6v1d*, *Vatp6v1h*, and *Pparα*, further confirming activation of TFEB by salinomycin (Fig. 8E). Taken together, the cell-based qHTS identifies Salinomycin as a potential TFEB agonist.

3.9. *Salinomycin protects against AILI in mice by activating hepatic TFEB*

Treatment with salinomycin markedly decreased levels of serum ALT and AST in mice after APAP overdose for 6 and 24 h (Fig. 9A and B). Consistent with the changes on the levels of serum ALT and AST, salinomycin treatment almost completely abolished the areas of centrilobular necrosis caused by APAP overdose, as shown by liver H&E and TUNEL staining (Fig. 9C and D). Results from the immunoblotting analysis showed that salinomycin treatment did not change the protein levels of CYP2E1. While APAP overdose reduced the protein levels of TFEB, treatment of salinomycin with APAP partially recovered hepatic TFEB levels. Furthermore, co-treatment of salinomycin reduced the levels of phosphorylated JNK after APAP overdose (Fig. 9E), which might contribute to its protection against APAP overdose. Taken together, salinomycin, which activated TFEB *in vitro*, significantly protected against APAP overdose in mice. Hepatic levels of APAP−protein adducts were similar in APAP-treated mice with or without salinomycin but salinomycin treatment markedly decreased serum levels of APAP-adducts (Fig. 9F and G), suggesting that salinomycin may promote the clearance of APAP-adducts in mice.

4. Discussion

Previous studies have demonstrated that activating of autophagy and lysosomal biogenesis is beneficial against AILI[7,10,31,32]. In the present study, there are several potential impactful findings and novelties that are worth highlighting. We used genetic loss-of and

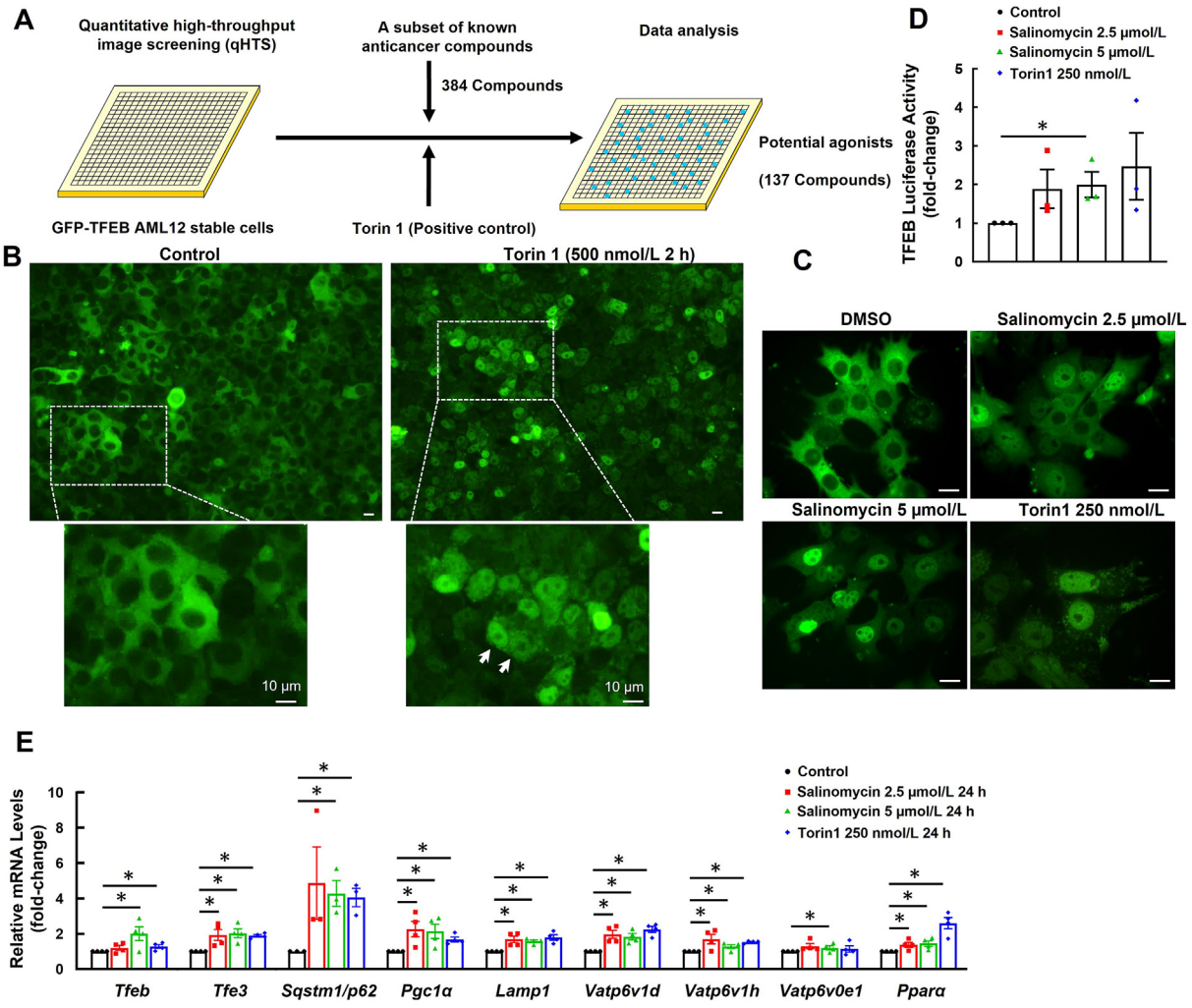

Figure 8 Quantitative high-throughput image screening for TFEB agonists in AML12 cells. (A) Schematic illustration of the cell-based quantitative high-throughput image screening for TFEB agonists/antagonists. (B) Stably expressing pEGFP-N1-TFEB AML12 cells were treated with DMSO or Torin1 at indicated concentration for 2 h. Representative microscopic images are shown. (C) Stably expressing pEGFP-N1-TFEB AML12 cells were treated with salinomycin or Torin1 at indicated concentration for 24 h. Representative confocal microscopic images are shown. (D) After transfection with pGL3-TFEB-Luc for 24 h, AML12 cells were treated with salinomycin or Torin1 at the indicated concentration for 24 h. TFEB-luciferase activity was determined. Data are mean ± SE ($n = 3$). *$P < 0.05$; Student's *t*-test. (E) Total mRNA was extracted followed by qPCR. Results were normalized to 18s and expressed as fold change compared to Control group. Data are mean ± SE ($n = 4$). *$P < 0.05$; Student's *t*-test.

gain-of function of hepatic TFEB approach and showed loss of hepatic TFEB exacerbated while overexpression of hepatic TFEB protected against AILI in mice, respectively. Mechanistically, increased TFEB may promote the clearance of APAP-adducts and increase mitochondria biogenesis as well as NRF2 activation with enhanced hepatic GSH synthesis. We also established an imaging-based qHTS platform for TFEB screening and identified salinomycin, an anti-bacteria agent, as a TFEB agonist in protecting against AILI in mice.

How does activation of TFEB protect against AILI? Autophagy may protect against AILI by removing APAP-adducts and damaged mitochondria after an acute overdose[6,11,31] and after multiple therapeutic doses[12]. While we found that serum ALT levels were tended to be higher in APAP-treated liver-specific *Tfeb* KO mice compared with matched WT mice, these changes did not reach the statistical significance. This could be due to low sample size and potential compensatory effects in liver-specific *Tfeb* KO mice as there are four TFEB family transcription factors (MiTF, TFEB, TFE3, TFEC)[15]. Narirutin (NR) a main bioactive constituent from a traditional Chinese medicinal herb, was recently reported to decrease hepatic APAP-adducts and AILI in mice by activating TFEB *via* enhanced calcineurin activity[32]. We also found that overexpression TFEB almost eliminated serum APAP-adducts and decreased levels of hepatic APAP adducts. These data indicate that increased clearance of APAP-adducts by increased TFEB-mediated lysosomal biogenesis may be one of the potential mechanisms in protecting against AILI.

It is generally thought that the pathogenesis of AILI has three phases: initiation, injury/progression and recovery/regeneration. However, the detail time course of the three phases could be varied in different strain of mice used and whether these mice are fed or fasted. Hepatic TFEB levels and the expression of TFEB target genes markedly decreased at 6 h but were gradually recovered at 24 h after APAP treatment, which is correlated with the severity of

Table 2 Potential TFEB agonists identified from the screen.

Name	AC_{50} (μmol/L)	Description
Sunitinib malate	1.66	An indolinone-based tyrosine kinase inhibitor with potential antineoplastic activity
Daunorubicin	1.66	Used for acute myeloid leukemia (AML), acute lymphocytic leukemia (ALL), chronic myelogenous leukemia (CML), and Kaposi's sarcoma
Idarubicin hydrochloride	1.87	Anthracycline antineoplastic antibiotic
Auranofin	2.35	An antirheumatic agent
Salinomycin	2.64	An antibacterial and coccidiostat ionophore therapeutic drug
Lasalocid sodium	6.05	An antibacterial agent and a coccidiostat
Nitazoxanide	6.62	A broad-spectrum antiparasitic and broad-spectrum antiviral drug
Hexadecyltrimethylammonium bromide	6.62	Used as an apoptosis-promoting anticancer agent for head and neck cancer (HNC)
Amsacrine hydrochloride	7.43	Used in acute lymphoblastic leukemia (ALL)
Nordihydroguaiaretic acid (Masoprocol)	7.62	An antioxidant and antineoplastic drug used to treat skin growths caused by sun exposure and prostate cancer
Pimozide	8.33	An antipsychotic drug, high potency compared to chlorpromazine (ratio 50:1−70:1)

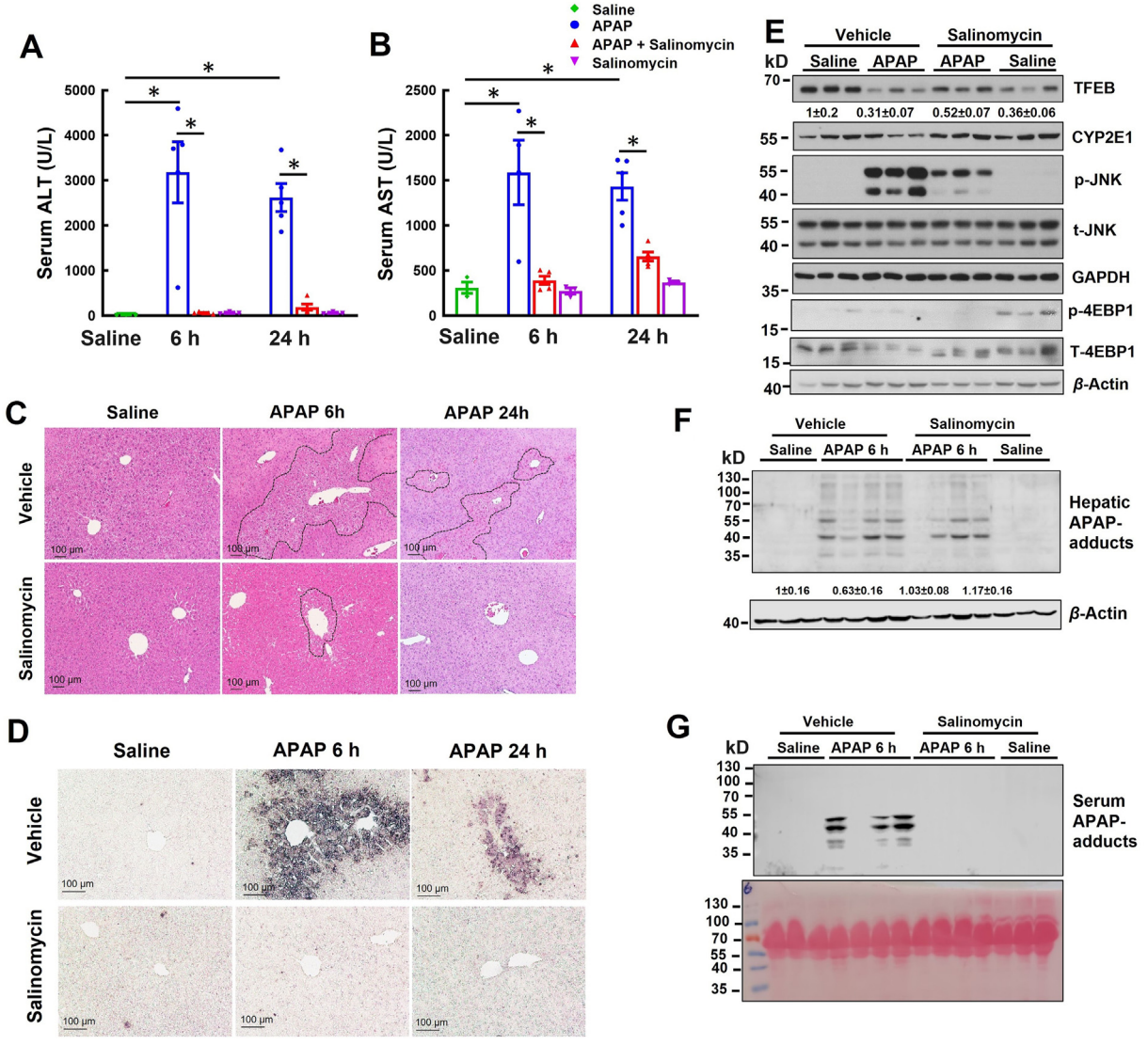

Figure 9 Salinomycin protects against APAP overdose-induced liver injury in mice. Male WT C57BL/6J mice were injected with acetaminophen (APAP, 500 mg/kg, i.p.) or saline for 6 and 24 h. Some mice were injected with salinomycin (5 mg/kg, i.p.) at the same time. 0.5% CMC-Na was used as vehicle control. (A) Serum ALT and (B) AST levels were quantified. Data are mean ± SE (n = 3−7). (C) Representative images of H&E staining are shown (magnification 100 ×). (D) Representative images of TUNEL staining are shown (magnification 200 ×). (E, F) Total liver lysates were subjected to Western blot analysis followed by densitometry analysis. Data are presented as mean ± SE (n = 3−4). (G) Mouse serum samples were subjected to Western blot analysis for APAP-adducts.

liver injury. The recovery of hepatic TFEB activity may also suggest that TFEB reactivation may be beneficial for liver regeneration/repair.

It is well documented that mitochondria damage is critical for APAP-induced hepatocyte necrosis. As a result, removal of damaged mitochondria *via* PARKIN−PINK1-mediated mitophagy or formation of mitochondria spheroids protects against AILI[6,31,33]. In addition to mitophagy, mitochondria biogenesis in liver zone 1 and 2 hepatocytes is also critical for AILI[33], which may be involved in hepatocyte proliferation and liver regeneration to promote recovery of AILI[9]. Overexpression of TFEB increased hepatic mitophagosome numbers, and the expression of PGC1α and TFAM as well as a group of mitochondrial genes, overexpression of TFEB increased PGC1α and TFAM as well as the expression of a group of mitochondrial genes, supporting a possible increased mitochondrial biogenesis by activation of TFEB in protecting against AILI.

Increased oxidative stress due to APAP metabolism and mitochondrial damage is a well-known mechanism of AILI, as the cytochrome P450-dependent formation of NAPDI is detoxified by GSH resulting in the depletion of GSH and formation of APAP-adducts[34,35]. Therefore, *N*-acetylcysteine (NAC), a precursor for GSH synthesis, scavenges NAPQI and attenuates the formation of APAP-adducts resulting in the protection against AILI[36]. NRF2 is a transcription factor that regulates a battery of genes on GSH synthesis and antioxidant genes against oxidative stress[37,38], which can be activated *via* canonical and non-canonical pathways[39,40]. Under normal conditions, NRF2 binds with Kelch-like ECH associated protein 1 (KEAP1), the latter recruits Cullin 3−ring box 1 (CUL3−RBX1) E3 ubiquitin ligase complex that ubiquitylates NRF2 resulting in degradation of NRF2 *via* the ubiquitin proteasome system[41,42]. In response to oxidative and electrophilic stress, several key cysteine residues in KEAP1 are modified resulting in the conformational change of NRF2−KEAP1 complex and prevention of NRF2 degradation[43]. Subsequently, NRF2 translocates to the nucleus and binds with sMAF to form a heterodimer to initiate the transcription[44]. In the non-canonical NRF2 pathway, p62, the substrate protein of autophagy, accumulates in autophagy defective cells[45,46]. p62 directly binds with KEAP1 *via* its KEAP1 interacting region (KIR) resulting in the release of NRF2 from KEAP1 followed by NRF2 stabilization and activation[47,48]. Indeed, liver-specific ATG5 KO mice have increased hepatic p62 accumulation and persistent NRF2 activation resulting in the resistance to AILI[45,49]. Interestingly, in the present study, we found *Sqstm1/p62* is a target gene of TFEB and overexpression TFEB increased hepatic expression of *Sqstm1/p62* and NRF2 activation, which may offer additional layer of protective mechanism against AILI by TFEB. NRF2 activation with induction of *Gclc* and *Gclm*, increases hepatic GSH synthesis, which is critical for peroxynitrite scavenging in the mitochondria during APAP hepatotoxicity[50]. Accelerated GSH re-synthesis after an APAP overdose was shown to be responsible for the reduced injury in female mice compared to male animals[51]; although endogenous IL-4 is a critical regulator of γ-*Gcl*[52], our data show that TFEB-mediated NRF2 activation is also a significant contributor to accelerated hepatic GSH synthesis and thus the protection caused by TEFB induction.

TFEB is mainly regulated at the posttranslational level. One of the well-studied mechanisms is the phosphorylation of TFEB by mTORC1 resulting in cytosolic retention and inactivation of TFEB. Therefore, mTORC1 inhibitors such as rapamycin and Torin 1 are potent TFEB agonists. However, mTORC1 inhibition can potentially lead to impaired cell proliferation and liver regeneration, which may counteract its beneficial effects on TFEB activation and autophagy induction. Indeed, mice with genetic loss of Raptor or mTOR did not show protection against AILI. Therefore, it is necessary to identify mTORC1-independent TFEB agonists to avoid the potential unwanted side effects on halting liver regeneration. To meet this need, we have identified a group of new TFEB agonists from the unbiased qHST screening using a subset library (383 drugs) of the NPC (The National Center for Advancing Translational Sciences (NCATS) Pharmaceutical Collection) containing 2816 approved or investigational drugs. Among them, salinomycin activated TFEB *in vitro* and *in vivo* with even higher mTORC1 activation in mouse livers. The mechanisms of how salinomycin activated TFEB independent of mTORC1 remain unclear. As discussed above, narirutin activated TFEB *via* increased calcineurin activation, the phosphatase that dephosphorylates TFEB[32]. Whether salinomycin would also affect calcineurin remains to be investigated in the future. Nonetheless, we also cannot rule out other possible off-target effects of salinomycin that may protect against AILI as the effects of TFEB activation in the mouse liver by salinomycin were not as profound as in cultured cells. Thus, the beneficial effects of salinomycin treatment in protecting against AILI may not necessarily be directly related to TFEB activation *in vivo*, which needs to be further studied in the future by using liver-specific *Tfeb* KO mice.

5. Conclusions

In summary, we found APAP overdose impaired hepatic TFEB and TFEB-mediated lysosomal biogenesis in mouse livers. Genetic manipulation of TFEB in mouse livers indicates a protective role of TFEB against AILI. More importantly, pharmacological activation of TFEB by salinomycin, a TFEB agonist identified from the high through-put screening, protected against AILI in mice. These findings support a potentially beneficial approach by targeting hepatic TFEB in protecting against AILI.

Acknowledgment

We would like to thank Dr. Thomas Rülicke at Department of Biomedical Sciences, University of Veterinary Medicine Vienna, Vienna, Austria and Dr. Kurt Zatloukal at The Institute of Pathology, Medical University of Graz, A-8036 Graz, Austria for providing us whole body Sqstm1/p62 knockout mice for the hepatocyte isolation experiment. We also thank Larysa Stroganova at University of Kansas Medical Center for her excellent assistance for the EM studies. This study was supported in part by the National Institute of Health (NIH, USA) funds R01 DK102142, R01 AG072895, R37 AA020518 (WXD) and in part by the Intramural Research Program of the National Center for Advancing Translational Sciences, NIH (USA).

Author contributions

Wen-Xing Ding conceived and supervised the project. Xiaojuan Chao, Mengwei Niu, Shaogui Wang, Xiaowen Ma, Xiao Yang, Hua Sun, Xujia Hu, Hua Wang, Ruili Huang, Li Zhang, Menghang Xia, and Hong-Min Ni performed experiments and analyzed the data. Hartmut Jaeschke, Andrea Ballabio, Hong-Min Ni and Wen-Xing Ding provided key reagents and intellectual discussions on experimental designs. Xiaojuan Chao and Wen-Xing Ding analyzed data and wrote the manuscript.

Conflicts of interest

A. Ballabio is co-founder of CASMA Therapeutics and Advisory board member of Next Generation Diagnostics and Avilar Therapeutics.

References

1. Chidiac AS, Buckley NA, Noghrehchi F, Cairns R. Paracetamol (acetaminophen) overdose and hepatotoxicity: mechanism, treatment, prevention measures, and estimates of burden of disease. *Expet Opin Drug Metabol Toxicol* 2023;**19**:297−317.
2. Long A, Magrath M, Mihalopoulos M, Rule JA, Agrawal D, Haley R, et al. Changes in epidemiology of acetaminophen overdoses in an urban county hospital after 20 years. *Am J Gastroenterol* 2022;**117**:1324−8.
3. Larson AM, Polson J, Fontana RJ, Davern TJ, Lalani E, Hynan LS, et al. Acetaminophen-induced acute liver failure: results of a United States multicenter, prospective study. *Hepatology* 2005;**42**:1364−72.
4. Jaeschke H, Adelusi OB, Akakpo JY, Nguyen NT, Sanchez-Guerrero G, Umbaugh DS, et al. Recommendations for the use of the acetaminophen hepatotoxicity model for mechanistic studies and how to avoid common pitfalls. *Acta Pharm Sin B* 2021;**11**:3740−55.
5. Jaeschke H, McGill MR, Ramachandran A. Oxidant stress, mitochondria, and cell death mechanisms in drug-induced liver injury: lessons learned from acetaminophen hepatotoxicity. *Drug Metabol Rev* 2012;**44**:88−106.
6. Williams JA, Ni HM, Haynes A, Manley S, Li Y, Jaeschke H, et al. Chronic deletion and acute knockdown of parkin have differential responses to acetaminophen-induced mitophagy and liver injury in mice. *J Biol Chem* 2015;**290**:10934−46.
7. Chao X, Wang H, Jaeschke H, Ding WX. Role and mechanisms of autophagy in acetaminophen-induced liver injury. *Liver Int* 2018;**38**:1363−74.
8. Ma X, McKeen T, Zhang J, Ding WX. Role and mechanisms of mitophagy in liver diseases. *Cells* 2020;**9**:837.
9. Du K, Ramachandran A, McGill MR, Mansouri A, Asselah T, Farhood A, et al. Induction of mitochondrial biogenesis protects against acetaminophen hepatotoxicity. *Food Chem Toxicol* 2017;**108**:339−50.
10. Ni HM, Bockus A, Boggess N, Jaeschke H, Ding WX. Activation of autophagy protects against acetaminophen-induced hepatotoxicity. *Hepatology* 2012;**55**:222−32.
11. Ni HM, McGill MR, Chao X, Du K, Williams JA, Xie Y, et al. Removal of acetaminophen protein adducts by autophagy protects against acetaminophen-induced liver injury in mice. *J Hepatol* 2016;**65**:354−62.
12. Nguyen NT, Akakpo JY, Weemhoff JL, Ramachandran A, Ding WX, Jaeschke H. Impaired protein adduct removal following repeat administration of subtoxic doses of acetaminophen enhances liver injury in fed mice. *Arch Toxicol* 2021;**95**:1463−73.
13. Qian H, Bai QY, Yang X, Akakpo JY, Ji LL, Yang L, et al. Dual roles of p62/SQSTM1 in the injury and recovery phases of acetaminophen-induced liver injury in mice. *Acta Pharm Sin B* 2021;**11**:3791−805.
14. Settembre C, Fraldi A, Medina DL, Ballabio A. Signals from the lysosome: a control centre for cellular clearance and energy metabolism. *Nat Rev Mol Cell Biol* 2013;**14**:283−96.
15. Chao X, Wang S, Zhao K, Li Y, Williams JA, Li T, et al. Impaired TFEB-mediated lysosome biogenesis and autophagy promote chronic ethanol-induced liver injury and steatosis in mice. *Gastroenterology* 2018;**155**:865−79.e12.
16. Settembre C, De Cegli R, Mansueto G, Saha PK, Vetrini F, Visvikis O, et al. TFEB controls cellular lipid metabolism through a starvation-induced autoregulatory loop. *Nat Cell Biol* 2013;**15**:647−58.
17. Settembre C, Di Malta C, Polito VA, Garcia Arencibia M, Vetrini F, Erdin S, et al. TFEB links autophagy to lysosomal biogenesis. *Science (New York, NY)* 2011;**332**:1429−33.
18. Medina DL, Di Paola S, Peluso I, Armani A, De Stefani D, Venditti R, et al. Lysosomal calcium signalling regulates autophagy through calcineurin and TFEB. *Nat Cell Biol* 2015;**17**:288−99.
19. Chao X, Wang S, Zhao K, Li Y, Williams JA, Li T, et al. Impaired TFEB-mediated lysosome biogenesis and autophagy promote chronic ethanol-induced liver injury and steatosis in mice. *Gastroenterology* 2018;**155**:865−79.
20. Wang S, Ni HM, Chao X, Wang H, Bridges B, Kumer S, et al. Impaired TFEB-mediated lysosomal biogenesis promotes the development of pancreatitis in mice and is associated with human pancreatitis. *Autophagy* 2019;**15**:1954−69.
21. Sun HH, McCracken J, Akakpo JY, Fulte S, Mckeen T, Jaeschke H, et al. Liver-specific deletion of mechanistic target of rapamycin does not protect against acetaminophen-induced liver injury in mice. *Liver Res* 2021;**5**:79−87.
22. Qian H, Chao X, Wang S, Li Y, Jiang X, Sun Z, et al. Loss of SQSTM1/p62 induces obesity and exacerbates alcohol-induced liver injury in aged mice. *Cell Mol Gastroenterol Hepatol* 2023;**15**:1027−49.
23. Lahiri P, Schmidt V, Smole C, Kufferath I, Denk H, Strnad P, et al. p62/sequestosome-1 is indispensable for maturation and stabilization of mallory-denk bodies. *PLoS One* 2016;**11**:e0161083.
24. Chao X, Wang S, Yang L, Ni HM, Ding WX. Trehalose activates hepatic transcription factor EB (TFEB) but fails to ameliorate alcohol-impaired TFEB and liver injury in mice. *Alcohol Clin Exp Res* 2021;**45**:1950−64.
25. Zhang ZY, Qian QW, Li MR, Shao F, Ding WX, Lira VA, et al. The unfolded protein response regulates hepatic autophagy by sXBP1-mediated activation of TFEB. *Autophagy* 2021;**17**:1841−55.
26. Huang R. A quantitative high-throughput screening data analysis pipeline for activity profiling. *Methods Mol Biol* 2016;**1473**:111−22.
27. Mansueto G, Armani A, Viscomi C, D'Orsi L, De Cegli R, Polishchuk EV, et al. Transcription factor EB controls metabolic flexibility during exercise. *Cell Metabol* 2017;**25**:182−96.
28. Klionsky DJ, Abdel-Aziz AK, Abdelfatah S, Abdellatif M, Abdoli Aabel S, Abel S, et al. Guidelines for the use and interpretation of assays for monitoring autophagy. *Autophagy* 2021;**17**:1−382.
29. Lim AY, Segarra I, Chakravarthi S, Akram S, Judson JP. Histopathology and biochemistry analysis of the interaction between sunitinib and paracetamol in mice. *BMC Pharmacol* 2010;**10**:14.
30. Wang Y, Mei X, Yuan J, Lu W, Li B, Xu D. Taurine zinc solid dispersions attenuate doxorubicin-induced hepatotoxicity and cardiotoxicity in rats. *Toxicol Appl Pharmacol* 2015;**289**:1−11.
31. Wang H, Ni HM, Chao XJ, Ma XW, Rodriguez YA, Chavan H, et al. Double deletion of PINK1 and Parkin impairs hepatic mitophagy and exacerbates acetaminophen-induced liver injury in mice. *Redox Biol* 2019;**22**:101148.
32. Fang ZY, Xu YY, Liu GW, Shao Q, Niu XD, Tai WJ, et al. Narirutin activates TFEB (transcription factor EB) to protect against Acetaminophen-induced liver injury by targeting PPP3/calcineurin. *Autophagy* 2023;**19**:2240−56.
33. Ni HM, Williams JA, Jaeschke H, Ding WX. Zonated induction of autophagy and mitochondrial spheroids limits acetaminophen-induced necrosis in the liver. *Redox Biol* 2013;**1**:427−32.
34. Jaeschke H, Ramachandran A. The role of oxidant stress in acetaminophe-induced liver injury. *Curr Opin Toxicol* 2020;**20−21**:9−14.
35. Mitchell JR, Jollow DJ, Potter WZ, Davis DC, Gillette JR, Brodie BB. Acetaminophen-induced hepatic necrosis. I. Role of drug metabolism. *J Pharmacol Exp Therapeut* 1973;**187**:185−94.
36. Corcoran GB, Racz WJ, Smith CV, Mitchell JR. Effects of *N*-acetylcysteine on acetaminophen covalent binding and hepatic necrosis in mice. *J Pharmacol Exp Therapeut* 1985;**232**:864−72.
37. Ma Q. Role of Nrf2 in oxidative stress and toxicity. *Annu Rev Pharmacol* 2013;**53**:401−26.
38. Dodson M, de la Vega MR, Cholanians AB, Schmidlin CJ, Chapman E, Zhang DD. Modulating NRF2 in disease: timing is everything. *Annu Rev Pharmacol Toxicol* 2019;**59**:555−75.

39. Dodson M, Zhang DD. Non-canonical activation of NRF2: new insights and its relevance to disease. *Curr Pathobiol Rep* 2017;**5**:171−6.
40. Ichimura Y, Waguri S, Sou YS, Kageyama S, Hasegawa J, Ishimura R, et al. Phosphorylation of p62 activates the Keap1−Nrf2 pathway during selective autophagy. *Mol Cell* 2013;**51**:618−31.
41. Zhang DD, Lo SC, Cross JV, Templeton DJ, Hannink M. Keap1 is a redox-regulated substrate adaptor protein for a Cul3-dependent ubiquitin ligase complex. *Mol Cell Biol* 2004;**24**:10941−53.
42. Kobayashi A, Kang MI, Okawa H, Ohtsuji M, Zenke Y, Chiba T, et al. Oxidative stress sensor Keap1 functions as an adaptor for Cul3-based E3 ligase to regulate for proteasomal degradation of Nrf2. *Mol Cell Biol* 2004;**24**:7130−9.
43. Zhang DD, Hannink M. Distinct cysteine residues in Keap1 are required for Keap1-dependent ubiquitination of Nrf2 and for stabilization of Nrf2 by chemopreventive agents and oxidative stress. *Mol Cell Biol* 2003;**23**:8137−51.
44. Itoh K, Chiba T, Takahashi S, Ishii T, Igarashi K, Katoh Y, et al. An Nrf2 small Maf heterodimer mediates the induction of phase II detoxifying enzyme genes through antioxidant response elements. *Biochem Bioph Res Co* 1997;**236**:313−22.
45. Ni HM, Boggess N, McGill MR, Lebofsky M, Borude P, Apte U, et al. Liver-specific loss of Atg5 causes persistent activation of Nrf2 and protects against acetaminophen-induced liver injury. *Toxicol Sci* 2012;**127**:438−50.
46. Pankiv S, Clausen TH, Lamark T, Brech A, Bruun JA, Outzen H, et al. p62/SQSTM1 binds directly to Atg8/LC3 to facilitate degradation of ubiquitinated protein aggregates by autophagy. *J Biol Chem* 2007;**282**:24131−45.
47. Komatsu M, Kurokawa H, Waguri S, Taguchi K, Kobayashi A, Ichimura Y, et al. The selective autophagy substrate p62 activates the stress responsive transcription factor Nrf2 through inactivation of Keap1. *Nat Cell Biol* 2010;**12**:213−23.
48. Lau A, Wang XJ, Zhao F, Villeneuve NF, Wu T, Jiang T, et al. A noncanonical mechanism of Nrf2 activation by autophagy deficiency: direct interaction between Keap1 and p62. *Mol Cell Biol* 2010;**30**:3275−85.
49. Ni HM, Woolbright BL, Williams J, Copple B, Cui W, Luyendyk JP, et al. Nrf2 promotes the development of fibrosis and tumorigenesis in mice with defective hepatic autophagy. *J Hepatol* 2014;**61**:617−25.
50. Saito C, Zwingmann C, Jaeschke H. Novel mechanisms of protection against acetaminophen hepatotoxicity in mice by glutathione and *N*-acetylcysteine. *Hepatology* 2010;**51**:246−54.
51. Du K, Williams CD, McGill MR, Jaeschke H. Lower susceptibility of female mice to acetaminophen hepatotoxicity: role of mitochondrial glutathione, oxidant stress and c-jun N-terminal kinase. *Toxicol Appl Pharmacol* 2014;**281**:58−66.
52. Ryan PM, Bourdi M, Korrapati MC, Proctor WR, Vasquez RA, Yee SB, et al. Endogenous interleukin-4 regulates glutathione synthesis following acetaminophen-induced liver injury in mice. *Chem Res Toxicol* 2012;**25**:83−93.